Journal of Engineering Research Innovation and Scientific Development 3 (3), (2025), 4-8 https://doi.org/10.61448/jerisd33252

Journal of Engineering Research Innovation and Scientific Development
journal homepage: www.jerisddelsu.com
Print ISSN 2971-6594 Online ISSN 2971-6608

Characterization and Classification of Coal Using Spectroscopic and Proximate Techniques: A Case Study of Coal from Azagba, Nigeria

M.U. Ajieh[1], R.N. Agbale[2], K. Owebor[3], L.O. Madagwu[4]

[1-2]*Department of Chemical Engineering, Delta State University, Abraka, Nigeria*
[3]*Department of Mechanical Engineering, Delta State University, Abraka, Nigeria*
[4]*National Agency for Science and Engineering Infrastructure (NASENI-NEDDI), Nnewi, Anambra State, Nigeria*

Corresponding author: *mike.ajieh@gmail.com (Ajieh M.U)

Article history: Received: 14-04-25, Revised: 17-06-25, Accepted: 20-06-25, Published: 21-06-25

Abstract

Nigeria's coal reserves remain largely underutilized in contrast to its more extensively developed oil and gas resources. The application potential of coal is influenced by its structural and chemical characteristics. This study focuses on the analysis of Azagba coal using various techniques, including X-ray fluorescence (XRF), X-ray diffraction (XRD), proximate and ultimate analyses, and Fourier-transform infrared spectroscopy (FTIR). Inorganic analysis reveals a dominant presence of SiO_3 (53.65%), SO_3 (16.18%), and Al_2O_3 (7.09%), indicating a siliceous composition. XRD analysis confirms a high proportion of graphite crystalline phase (82%) and minerals such as quartz, marialite, and calcite. Key structural indicators—interlayer spacing (d002 = 3.38 Å) and stacking height (Lc = 57.32 nm)—suggest a well-ordered carbon framework. FTIR spectra further reveal hydroxyl (-OH), aliphatic (C-H), and various oxygen-containing groups, with a high aromatic hydrogen ratio (Hal/H = 0.49) and significant aromaticity (fa = 0.68). The proximate and ultimate analyses classify Azagba coal as a high-rank, volatile bituminous to anthracite type, marked by a high fixed carbon content (59.47%) and low ash content (1.13%). These attributes emphasize the coal's structural maturity, reactivity potential, and industrial applicability.

Keywords: Demineralization; Characterization; Crystalline; Aromaticity; Aliphatic; Analysis; Peak

1. Introduction

Energy security forms the foundation for economic advancement and social progress (Ezemonye et al., n.d.). The rapid pace of urbanization, industrialization, and global population growth has significantly increased energy demand. It is projected that worldwide energy consumption will rise by 40% between 2015 and 2030 (Kavouridis & Koukouzas, 2008). This trend underscores the need to explore and utilize all available energy sources—both renewable and non-renewable—to satisfy the growing demand.

Coal, the most abundant fossil fuel on Earth, is a non-renewable energy source and the most cost-effective, providing energy at roughly one-third the price of oil or natural gas per energy unit (Yan et al., 2020). It is an organic sedimentary rock formed through the metamorphic transformation of peat and other biological residues within the Earth's crust (Jie et al., 2021). Typically, black or brownish-black in colour, coal is primarily composed of carbon and hydrocarbons, making it a key raw material for energy production. Currently, coal-fired power plants account for approximately 36% of global electricity generation (IEA, 2024) (Chen & Xu, 2010; Ghose, 2009; Peteves et al., 2007). Remarkably, global coal capacity rose from 550.6 GW to 578.2 GW in 2024, representing a 5% growth largely driven by China's expansion efforts (Clark et al., 2020)

Historically, coal has served as a vital energy source, widely used for electricity and heat generation, as well as in various industrial applications such as cement production, iron and steel manufacturing, and as a raw material for liquid fuels. According to the International Energy Agency (IEA, 2024), coal will remain essential for iron and steel production until alternative technologies are developed. Coal reserves are plentiful worldwide, with China and the United States leading in global reserves, although most countries possess accessible deposits. The widespread use of coal for electricity generation has significantly contributed to socio-economic advancement, infrastructure development, and poverty reduction (Oboirien et al., 2018; Oseni, 2011). Despite these benefits, coal remains the largest anthropogenic contributor to global carbon dioxide emissions (IEA, 2024).

Africa contributes minimally to global greenhouse gas emissions, accounting for less than 3% of the world's total carbon dioxide output (UN Fact Sheet on Climate, 2006). In line with this, the World Resources Institute reported that in the year 2000, Africa's per capita CO_2 emissions were approximately 0.8 metric tons, significantly lower than the global average of 3.9 metric tons per person. Despite this, the continent aims to adopt balanced strategies that harness its natural resources—such as coal—to address rising energy demands while simultaneously embracing cleaner technologies to reduce environmental impact. Although clean coal technologies are a step toward achieving the goals of the Paris Agreement, hydrogen derived from such methods is increasingly seen as a viable, affordable, and sustainable energy source, aligning with the objectives of Sustainable Development Goal 7 (SDG7) even beyond 2030.

Nigeria, within Sub-Saharan Africa, holds one of the region's most substantial coal reserves, with estimated total deposits of 2.5 billion tonnes and proven reserves of about 200 million tonnes (Oseni, 2011). In addition to the relatively low production costs associated with coal compared to other fossil fuels, advancements in mining technology have made its extraction more efficient. Coal's low market price also enhances its processing viability relative to crude oil or natural gas. Globally, coal contributed around 38.1% to electricity generation in 2017, reinforcing its role as a major energy source (Chang et al., 2016; Clark et al., 2020; Pudasainee et al., 2020a). Moreover, coal is chemically diverse, consisting of a complex matrix of organic structural units bound by covalent and noncovalent interactions of varying magnitudes. Key molecular structures within coal include fused aromatic and hydroaromatic rings, which often incorporate heteroatoms like sulfur, oxygen, and nitrogen. This structural complexity necessitates the use of various analytical techniques to accurately evaluate and characterize its chemical composition (He et al., 2017; Hou et al., 2017).

The advancement of modern technologies presents opportunities for substantial reductions in greenhouse gas emissions and capital costs associated with coal-based systems, while also enhancing thermal efficiency and operational reliability (Franco & Diaz, 2009; Melikoglu, 2018; Norouzi et al., 2020). Recent studies on clean coal technologies highlight coal's potential as a viable source of hydrogen energy. Despite coal's notable contribution to greenhouse gas emissions and its impact on climate change, progress in gasification technology indicates that coal can achieve lower emission levels compared to oil and natural gas fuels (Melikoglu, 2018; Norouzi et al., 2020; van der Zwaan, 2005; Yegulalp et al., 2001).

Moreover, coal reserves have the potential to last for centuries—far exceeding the lifespan of oil and gas resources. With the advancement of environmentally friendly coal technologies, integration with conventional coal-fired power plants can achieve high energy conversion efficiency, lower emissions, and reduced particulate matter (Franco & Diaz, 2009; Norouzi et al., 2020). Additionally, advanced gasification techniques have demonstrated significant promise for hydrogen (H_2) production, enabling carbon dioxide (CO_2) sequestration and minimizing emissions of pollutants such as sulfur oxides (SOx) and nitrogen oxides (NOx), offering a cleaner alternative to traditional coal-based electricity generation methods (Yan et al., 2020).

Coal possesses the lowest hydrogen-to-carbon ratio, indicating that its utilization results in greater CO_2 emissions per mole of H_2 produced (Ghose, 2009; Shoko et al., 2006; Stiegel & Ramezan, 2006; Zhang et al., 2017a). Despite this, low-rank coal offers several advantages, including high volatile matter content, enhanced reactivity, lower extraction costs, and reduced concentrations of pollutants such as sulfur, nitrogen, and heavy metals. Additionally, low-rank coal generally contains a higher hydrogen content (Reddy & Vinu, 2016). Notably, gasification presents an opportunity to produce hydrogen with high purity and efficiency (Chang et al., 2016; Takeshita & Yamaji, n.d.).

Nigeria faces a significant energy access deficit, while its steel industry remains largely inactive. Despite these challenges, the country possesses substantial coal reserves that present an opportunity for hydrogen production. However, while sufficient research on coal utilization for energy generation abounds, there is limited literature on the classification of coal using its unique structure, chemical heterogeneity and rank, especially for Nigerian-derived coal. Therefore, this

study focuses on evaluating the physicochemical and thermal properties of coal from the Azagba mine in Delta State, Nigeria. The overarching goal is to support the revitalization of the Nigerian coal industry for improved energy outcomes when subjected to advanced technologies such as Integrated Gasification Combined Cycle (IGCC) and Integrated Gasification Fuel Cell (IGFC) systems (Chang et al., 2016; Clark et al., 2020; Norouzi et al., 2020). Essentially, research of this nature in Nigeria is novel as Delta State is not a renowned location unlike Enugu and other states for coal mining. This suggests that more discoveries of coal deposits are expected to increase to support existing energy resources. Nonetheless, with growing technological advancements and international pressure to reduce greenhouse gas emissions and other pollutants, the deployment of IGCC and IGFC technologies could become both technically viable and economically sustainable, paving the way for cleaner and more environmentally friendly energy solutions (Ajieh et al., 2023; Shoko et al., 2006).

2. Materials and Methods

2.1 Sample preparation and Analysis

The coal sample used in this study was sourced from Azabga-Ogwashi (6°14′33.7″N, 6°35′42.3″E), Delta State, Nigeria. To eliminate surface impurities, the coal was thoroughly rinsed with distilled water until the wash water ran clear. It was then dried in a vacuum oven at 105 °C for 24 hours and subsequently crushed to a particle size smaller than 60 mesh for further analysis. Proximate analysis was performed on a mass basis to determine the proportions of fixed carbon, moisture content, volatile matter (the gases released during thermal decomposition in an inert atmosphere), and ash (the inorganic residue post-combustion). Moisture content, evaluated using ASTM D3173, affects the efficiency of combustion by increasing heat loss through vaporization and superheating. To determine moisture content, an empty crucible was first weighed, after which 1 gram of pulverized coal was added. The total weight of the crucible and sample was recorded. The crucible was then gently tapped to evenly distribute the sample across the base and placed in an oven set between 105 °C and 110 °C for one hour. After heating, the crucible was cooled in a desiccator and reweighed. Moisture percentage was calculated using Equation 1:

$$\text{Moisture Content (wet basis)} = \frac{(W_1 - W_2)}{W_1} \times 100\% \quad (1)$$

where W_1 represents the mass of the original sample and W_2 denotes the mass after drying.

Ash content, as defined by ASTM D3174, refers to the non-combustible residue left after burning, which is considered an impurity. It negatively impacts fuel handling and combustion efficiency by increasing operational costs, contributing to clinkering and slagging, and reducing overall boiler performance. To determine ash content, the sample was heated to 750 °C and held at that temperature for one hour to ensure complete combustion of all volatile components. Afterwards, the crucible was removed from the furnace, allowed to cool for about a minute in ambient laboratory conditions, and then placed in a desiccator to reach room temperature. The residue was weighed again, and the ash content was calculated using Equation 2:

$$\%\,\text{Ash} = \frac{\text{Mass of residue after combustion}}{\text{Mass of original sample}} = \frac{(W_1 - W_2)}{W_1} \times 100\% \quad (2)$$

Volatile matter, as defined by ASTM D3175, includes components such as methane, hydrocarbons, hydrogen, carbon monoxide, and non-combustible gases like carbon dioxide and nitrogen found in coal. It serves as an indicator of the coal's gaseous fuel content, contributing to longer flame length, easier ignition, and influencing furnace design parameters such as height, volume, and secondary air requirements. To determine volatile matter, an empty crucible with a lid was first weighed. Approximately 1 gram of the blended coal sample was added, and the crucible with its contents was weighed again. The sample was gently leveled at the base of the crucible. It was then preheated to 955 °C and maintained at that temperature for exactly seven minutes. Afterward, it was cooled for one minute at room temperature, placed in a desiccator to fully cool, and reweighed. It is important to note that the volatile matter reported in proximate analysis excludes moisture, although both moisture and volatiles are expelled during heating. The volatile content was computed using Equation 3:

$$\%\,\text{Volatiles} = \frac{(W_2 - W_3)}{W_2 - W_1} \times 100\% - M \quad (3)$$

where W_1 is the mass of the empty crucible and lid, W_2 is the mass of the crucible, lid and sample before heating, W_3 is the mass of the crucible, lid and sample after heating, and M is the % moisture content. Furthermore, fixed carbon, as defined by ASTM D3172, refers to the solid residue remaining in the furnace after the volatile matter has been expelled. While it is primarily composed of carbon, it also contains small amounts of hydrogen, oxygen, sulfur, and nitrogen that are not released during heating. Fixed carbon provides an approximate measure of the coal's heating value and is determined using Equation 4:

$$\%\,\text{Fixed Carbon} = 100 - (\%\,\text{moisture} + \%\,\text{volatiles} + \%\,\text{ash}) \quad (4)$$

The fixed carbon and volatile content on a dry, ash-free basis, i.e. ignoring the moisture and ash content, can be calculated from Equations 5 and 6, respectively;

$$\%\,\text{Fixed Carbon (dry, ash-free)} = \frac{\text{Measured fixed carbon}}{\text{Fixed carbon + Volatiles}} \times 100\% \quad (5)$$

$$\%\,\text{Volatiles (dry, ash-free)} = \frac{\text{Measured Volatiles}}{\text{Fixed carbon + Volatiles}} \times 100\% \quad (6)$$

In addition, ultimate analysis was conducted to determine the elemental composition of the coal sample, including carbon, hydrogen, oxygen, sulfur, and others. The analysis was performed using the LECO CHNS 2000 Elemental Analyzer in line with ASTM 3174-76, a standard method for the instrumental determination of carbon, line, and nitrogen. This analysis is essential for estimating the amount of air needed for combustion, as well as the volume and composition of the resulting combustion gases. Such data are critical for calculating flame temperature, conducting material balance calculations, and supporting various design applications.

2.2 Characterization of coal

The composition of inorganic elements in the coal sample was determined using X-ray fluorescence (XRF). A thin film of propylene was applied to the sample container to ensure a smooth surface. Approximately 5 g of pulverized coal was placed into a film-covered sample cup, filling it to about one-third of its volume. The lid was securely sealed to prevent any leakage or disturbance of particles on the film surface. The prepared sample was then placed in the sample turret of the Genius-IF xenometric XRF chamber. The X-ray lamp was powered on and allowed to stabilize for 2 minutes before initiating the analysis. Pre-calibration and verification of the instrument were conducted to determine the precision and accuracy.

X-ray diffraction (XRD) analysis was employed to examine the crystalline structure of the sample. The technique evaluates diffraction peak characteristics—such as position, intensity, and shape—using the Rigaku MiniFlex 600 XRD diffractometer, which is essential for phase identification and quantitative analysis. This method provides detailed insights into crystal morphology, particle size, and orientation. The system was powered via the control panel, with the voltage and current set to 30 kV and 15 mA, respectively, and the temperature maintained between 21–23 °C. Once the system was powered and verified, the coal sample was finely ground and homogenized and the average bulk composition was determined. It was then compressed into a flat, smooth surface using a sample preparation block and mounted on the sample stage inside the XRD unit.

Key structural parameters were derived by analyzing peak positions and full widths at half maximum intensity using empirical equations, including the Scherrer formula. The Bragg equation (see Equation 7) was applied to determine the interlayer spacing (d_{002}) between aromatic layers (Li et al., 2015).

$$d_{002} = \frac{\lambda}{2 \sin \theta_{002}} \quad (7)$$

The average crystallite stacking height (L_c) was calculated using Equation 8,

$$L_c = \frac{0.89\lambda}{\beta_{02} \cos \theta_{002}} \quad (8)$$

The average diameter of coal crystallites is represented in Equation 9,

$$L_c = \frac{1.84\lambda}{\beta_{02} \cos \theta_{002}} \quad (9)$$

The average number of crystallites in a stack (N_{ave}) was computed using Equation 10

$$N_{Av} = \frac{L_c}{d_{002}} \quad (10)$$

The aromaticity of the coal was determined based on Equation 11,

$$f_{ar} = \frac{A_{002}}{A_{002} + A_\gamma} = \frac{c_{ar}}{c_{ar} + c_{al}} \quad (11)$$

The coal rank was evaluated using Equation 12,

$$I = I_{002} / I_\gamma \quad (12)$$

where λ is the X-ray wavelength, determined by the radiation source (0.1542 nm for Cu Kα radiation), β_{02} represents the full width at half maximum (FWHM) of the (002) diffraction peak in radians, and Θ_{002} is the Bragg angle corresponding to the (002) peak, also in radians. A_{002} and Aγ denote the integrated areas of the (002) and γ diffraction peaks, respectively. These areas correspond to the proportions of aromatic carbon atoms (C_{ar}) and aliphatic carbon atoms (C_{al}) present, as reported by (Jiang et al., 2019a). Additionally, I_{002} is the intensity of the (002) diffraction peak, which reflects the presence of well-aligned aromatic layers, while I_λ corresponds to the intensity of the λ band, indicating non-crystalline carbon structures.

Furthermore, functional groups of the organic and inorganic compounds present in the coal sample were identified using a Shimadzu Fourier Transform Infrared Spectrophotometer (FTIR 8400S). For the analysis, coal samples were weighed and thoroughly mixed with 0.01 g of anhydrous KBr using a mortar and pestle. The resulting mixture was compressed into a transparent pellet using a vacuum hydraulic press (Graseby Specac) at 1.2 psi. The pellet was scanned in the infrared range of 400–4000 cm^{-1}, and the absorption data were recorded digitally. The average number of crystallites in a stack (N_{ave}) was calculated using Equation 13;

$$N_{Av} = \frac{L_c}{d_{002}} \quad (13)$$

The aromaticity of the coal was determined using Equation 14;

$$f_{ar} = \frac{A_{002}}{A_{002}+A_{\gamma}} = \frac{c_{ar}}{c_{ar}+c_{al}} \quad (14)$$

The coal rank was evaluated from Equation 15:

$$I = I_{002} / I_{\gamma} \quad (15)$$

where λ is the X-ray wavelength, determined by the radiation source (0.1542 nm for Cu Kα mode used), β_{002} is the full width at half maximum (FWHM) of the (002) diffraction peak in radians, and Θ_{002} is the Bragg angle corresponding to the (002) peak (in radians). A_{002} and Aγ represent the integrated areas of the (002) and γ peaks, respectively. These areas correspond to the quantities of aromatic carbon atoms (C_{ar}) and aliphatic carbon atoms (C_{al}), respectively (Jiang et al., 2019a). Essentially, I_{002} denotes the intensity of the (002) diffraction peak, which reflects the degree of order in the stacked aromatic layers, while I_{λ} refers to the intensity of the λ band, associated with non-crystalline carbon.

Additionally, parameters from proximate and ultimate analyses were used to compute the apparent aromaticity, the ratio of aliphatic to total hydrogen, and the number of aromatic carbon rings in the monomer. The apparent aromaticity was determined using Equation 16:

$$f_a = (100 - v) \times \frac{0.9677}{c} \quad (16)$$

where v is the volatiles and C is the carbon content. The value 0.9677 is the fitting coefficient typical for coal (Jiang et al., 2019b). Equation 17 represents the ratio of aliphatic hydrogen to total hydrogen:

$$H_{al} / H = (1 - f_a)(C / H)\left(H_{al} / C_{a_l}\right) \quad (17)$$

For most coal, the ratio H_{al}/C_{al} is given as 0.18 (Kavouridis & Koukouzas, 2008)

The equation for the determination of the number of aromatic carbon rings in a single monomer was proposed by Kastner and is shown in Equation 18;

$$(R / C)_u = 1 - \frac{f_a}{2} - \frac{(H/C)}{2} \quad (18)$$

2.3 Structural Analysis

The aliphatic chain length was determined using Equations 19 - 21 in accordance with (Jiang et al., 2019b; K. Li et al., 2015).

$$\frac{H_{al}}{H} = \frac{H_{al}}{H_{al}+H_{ar}} = \frac{A_{2920-2851}}{A_{2920-2851}+A_{1626}} \quad (19)$$

$$f_a = 1 - \frac{c_{al}}{c}$$

where $\frac{c_{al}}{c} = \left(\frac{H_{al}}{H} \times \frac{H}{c}\right) / \frac{H_{al}}{c_{al}}$

$$\frac{CH_2}{CH_3} = \frac{A_{2920}}{A_{2851}} \quad (20)$$

$$\left(\frac{R}{c}\right)_u = 1 - \frac{f_a}{2} - \frac{H}{C}$$

The aromaticity and rank of the coal was determined using Equation 21,

$$\frac{A_{ar}}{A_{al}} = \frac{A_{1626}}{A_{2920}+A_{2851}} \quad (21)$$

3. Results and Discussions

3.1 Inorganic composition of coal

Table 1 presents the oxide composition of various inorganic elemental species found in the coal sample. The primary inorganic minerals in the coal are SiO_2 (53.65%), SO_3 (16.18%), Al_2O_3 (7.09%), Cl (6.42%), Fe_2O_3 (5.53%), and CaO (3.18%). The significant presence of SiO_2, Al_2O_3, and Fe_2O_3 indicates the siliceous nature of the coal, supporting the findings (Rawat & Yadav, 2019) who reported that these three oxides make up 90% of the inorganic oxides, with SiO_2 accounting for 63.04%. Hazra (Hazra et al., 2025) characterized selected Indian shales and found, SiO_2, Al_2O_3, and Fe_2O_3 contents ranged from 67.26 to 65.89%, 18.92 to 26.19%, and 4.55 to 10.58%, respectively, across all shale types studied. The elevated levels of SO_2 (16.18%) and Cl (6.42%) suggest high sulfur and chlorine content. Similarly. Zhang (Zhang et al., 2017b) noted that SiO_2 content in coal before demineralization ranged from 9.86% to 10.70%. The CaO content (3.18%) in this coal is moderately high, which may contribute to improved combustion through catalytic activity (Gao et al., 2017a; Qiao et al., 2022).

Table 1: Composition of Inorganic Oxides in Test

Oxides of elements	Concentration %
SiO_2	53.65
SnO	2.55
TiO_2	0.52
V_2O_5	0.09
Cr_2O_3	0.066
MnO	0.22
Fe_2O_3	5.53
Co_3O_4	0.096
NiO	0.043
CuO	0.35
WO_3	0.001
P_2O_5	0.00
SO2	16.18
CaO	3.18
MgO	0.00
K_2O	0.43
BaO	0.14
Al_2O_3	7.09
Ta_2O_5	0.0041
ZnO	0.33
Ag_2O	0.03
Cl	6.42
ZrO_2	0.05

The XRD spectra of Azagba coal, shown in Figure 1, predominantly feature a graphite phase, a form of crystalline carbon that constitutes 82% of the total crystallites. Other crystalline phases identified include quartz, which confirms the presence of SiO_2, and marialite, indicating the presence of Cl. Additionally, the coal sample contains crystalline phases of calcite, illite, and pyrite, which can be attributed to the CaO, SiO_2, and SO_2 components of the coal. The results from the Gaussian peak curve fitting reveal that the (γ) band appears around 17°. The peaks at 2θ = 28.07° and 43° observed in the coal samples are associated with the crystalline structures in the π-band (002) and 100 band, as shown in Table 2.

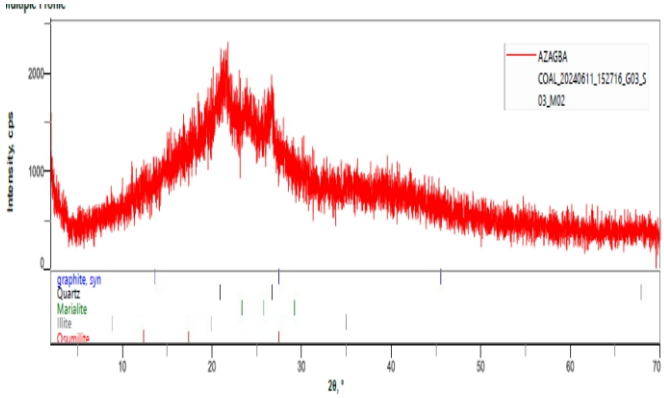

Figure 1: X-ray Diffraction of Test Coal

The (002) and (10) bands exhibit significant intensity. Additionally, the high background signal indicated a significant presence of amorphous material, suggesting a combination of ordered and disordered phases in its composition.

Table 2: Structural parameters of coal determined from XRD analysis

d_{002} (nm)	L_c (*nm*)	L_d (nm)	N_{av}	f_{ar}	I
3.38	5.73	7.90	31.16	0.72	0.31

The γ band, observed between 15° and 19°, is typically associated with saturated carbon structures in coal, particularly due to the presence of long aliphatic chains within crystallites [28]. The characteristic parameters, including aromaticity (fa), interlayer spacing (d002), layer stacking height (Lc), lateral diameter (La), and crystallite volume (Vc), were determined by curve-fitting the γ and π-bands. The aromaticity (fa) value was found to be 0.72, indicating a high level of aromaticity. The stacking height (Lc) of the layers was 57.32 nm, and the lateral diameter (La) was 79.03 nm. The interlayer spacing (d002) value was 3.38 Å. The high fa value indicates that the coal has a significant aromatic content and a low aliphatic component, suggesting it is a high-rank coal. The d002 value is close to that of graphite, which has d002 values in the range of 3.36–3.37 Å (Jiang et al., 2019b). Additionally, the values of Lc and La suggest the coal has a well-developed structural stacking and ordering, characteristics typically associated with high-rank coals. These findings indicate that Azagba coal is likely to be a highly volatile bituminous coal (Gao et al., 2017a; Okolo et al., 2015a). The high graphite concentration (82%) in the crystallites further supports this and suggests that Azagba coal belongs to the meta-bituminous to anthracite class, indicating it is a medium-ranked, mature coal (R. Li et al., 2022)

Nonetheless, the ultimate analysis (CHNS) and that of proximate analysis (i.e., fixed carbon, moisture and ash composition) are shown in Table 3 and further tested with the modified Dulong model to unravel the high heating value of coal as shown in Equations 22 (Jie et al., 2021; Peteves et al., 2007)

$$HHV = 81C + 342.5\left(H - {}^{O}/_{8}\right) + 22.5S - 6(9H - W) \quad (22)$$

The results indicate that the coal consists of 23.26% volatile matter with carbon content (74.65%), fixed carbon (59.47%) and High Heating Value (HHV) of 29MJ/kg are characteristic of high-rank coal (Jie et al., 2021). This further shows that the coal has a low ash content (4.13%) and moderate volatile matter (23.26%), which reflects the transformation of combustible substances into stable materials during the coalification process (Zhang et al., 2017a). The moisture content of 12.47% is typical for bituminous coal. With a H/C ratio of 0.07, the coal is classified as a higher-rank material, likely falling between bituminous and anthracite. The O/C ratio of 0.28 further supports its bituminous classification, suggesting it is of medium rank (Gao et al., 2017b). This may be

due to the advanced maturation of the coal with a high energy content (Pudasainee et al., 2020b). The aromatic ratio (fa) of 0.72 is relatively high, indicating mature coal, with most aliphatic substances removed during coalification. The (R/C)u ratio, representing the degree of aromatic ring condensation, is 0.28, indicating significant condensation of the aromatic structures. Despite the coal's high aromaticity, the aromatic clusters are not tightly fused, suggesting a rich availability of reactive sites for chemical processes (Banerjee et al., 2019). The structural parameters of the coal sample are as shown in Table 4.

Table 4: Parametric Structures of FTIR Spectra of Coal Sample

Parameter	H_{al}/H	f_a	CH_2/CH_3	$(R/C)_u$	Ar/A_{al}
	0.70	0.68	1.09	0.25	0.43

The structures and functional groups of coal absorption peaks are typically categorized into four main regions: hydroxyl functional groups (3000-3600 cm^{-1}), aliphatic structures (2700-3000 cm^{-1}), aromatic structures and O_2 -containing functional groups (1000–1800 cm^{-1}), and aromatic structures with low wavenumber and minerals (400–900 cm^{-1}) (Yang & Qiu, 2019). The peaks which corresponded to functional groups (the different vibrations of the functional groups) present were shown in the infrared section of the electromagnetic spectra between a wavelength of 4000 and 600 cm^{-1} (Clark et al., 2020), as shown in Figure 2.

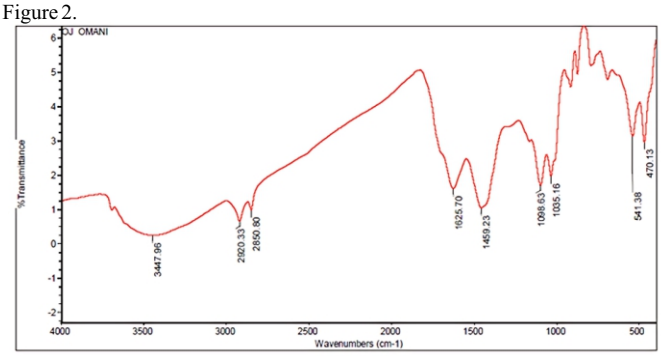

Figure 2: FTIR spectra of Coal Sample

The medium sharp peaks at 3447.96 and 3570 cm^{-1} are attributed to the stretching vibrations of -OH groups, indicating the presence of moisture. The peak around 2992 cm^{-1} is due to the CH_2 stretching vibrations in aliphatic chains (Costa & Paranhos, 2020). The stretching vibration at 1625.70 cm^{-1} suggests the presence of oxygen-containing functional groups such as phenols, alcohols, ethers, carboxylic acids, carbonyls, and NO_2 in the coal. Peaks between 541.38 and 470.13 cm^{-1} are likely related to Si-O stretching and Si-O-Si bending vibrations, pointing to the presence of quartz, as confirmed by XRD analysis and the high SiO_2 content identified by XRF analysis.

The content of aromatic hydrogen (Hal/H) was found to be greater than that of aliphatic hydrogen, with a value of 0.49. The aromaticity (fa) was calculated to be 0.68, indicating that a substantial portion of the coal's carbon is aromatic, correlating with the high fixed carbon content observed in the proximate analysis. The fa values derived from XRD and elemental analysis closely matched those obtained from FTIR analysis, with slight differences attributed to variations in the analytical methods used. Similarly, (Jiang et al., 2019b) investigated the molecular structural characteristics of Vitrinite and Inertinite from Bituminous Coal using FTIR (Micro-Raman) and XRD Spectroscopy, finding fa values for raw coal ranging from 0.72 to 0.92. This was corroborated by (J. Yan, Lei, et al., 2020), with fa values for low-rank coal falling between 0.63–0.90, 0.47–0.72, and 0.34–0.73 based on FTIR, NMR, and XRD analyses, respectively. Furthermore, (Okolo et al., 2015b) found fa values ranging from 0.72 to 0.82.

The CH_2/CH_3 ratio of 1.09 indicates a significant presence of methylene groups, suggesting that the coal contains substantial aliphatic chains, although the aliphatic components are less abundant than the aromatic ones (J. Yan, Yang, et al., 2020).

The Azagba coal shows a high degree of aromaticity, supported by its elevated Hal/H and fa values (see Table 4). The aromatic structures have relatively few aliphatic groups attached, leading to low (R/C)u ratios. While aliphatic components are present, they are less prevalent compared to aromatic materials, as evidenced by the moderate CH_2/CH_3 and Ar/Aal ratios. The indication of longer aliphatic chains ($CH_2/CH_3 > 1$) suggests that these components are primarily composed of straight or branched chains rather than small alkyl groups attached to the structure, as shown in Table 5.

Table 3: Ultimate and proximate analysis

Ultimate						Proximate								
C (%)	H (%)	N (%)	S	O	MC	Dry matter	Ash	FC	volatiles	H/C	O/C	f_a	H_{al}/H	$(R/C)_u$
74.65	5.16	0	4.42	15.77	12.47	96.26	4.13	59.47	23.26	0.07	0.28	0.65	0.40	0.31

Table 5: Characteristics of Coal Sample

S/N	Wavelength	Transmittance	Assignment of functional group	Intensity of peaks
1.	3447.96	0.252	O–H Stretching (Hydroxyl groups, Alcohols, Phenols)	Strong and broad
2.	2920.22	0.657	C–H Stretching (Aliphatic CH_2)	Medium Asymmetric stretching
3.	2850.80	0.993	C–H Stretching (Aliphatic CH_3)	medium Stretching
4.	1625.70	1.61	C=C Stretching (Aromatic rings, Quinones)	medium
5.	1459.23	1.05	C–H Bending (Aliphatic CH_2 and CH_3 groups)	Medium stretch Deformation vibration
6.	1098.83	1.703	C–O-C Stretching Deformation od phenol	strong
7.	1035.16	1.978	S=O Stretching (from sulphurdine	strong
8.	541.38	3.14	Out-of-plane Bending Si-O, Al-O-Si,	Aromatic ring substitution pattern
9.	470.13	2.958	Out-of-plane Deformation Si-O-Si,	Ring bending vibration

4. Conclusion

The coal sample from the Azagba deposit was analyzed for its structural characteristics using various analytical techniques. XRF analysis indicated that the coal is siliceous and contains a relatively high amount of calcium carbonate. The presence of SO_2 at 16.3% suggests that desulphurization may be necessary before its use. XRD analysis revealed that the crystalline phase of the coal consists of 82% graphite, with high graphitization supported by a well-ordered crystalline structure. The interlayer spacing (d002) was measured at 3.38 Å, and the stacking height (Lc) was 57.32 nm, values typical of graphite. The coal's apparent aromaticity, as determined from XRD, proximate analysis, and FTIR, ranged from 0.65 to 0.72. The proximate and ultimate (CHNS) analyses show that the coal is a high-rank, volatile bituminous to anthracite coal, with a high fixed carbon content of 59.47% and a low ash content of 1.13%. The high aromatic content and low aliphatic hydrogen ratio suggest enhanced thermal stability and advanced coalification. FTIR spectroscopy confirmed the presence of hydroxyl groups (-OH), aliphatic (-CH_2,- CH_3), and aromatic C=C bonds. The CH_2/CH_3 ratio of 1.09 supports the presence of long-chain aliphatic structures and further indicates the coal's high rank. In summary, the Azagba coal sample is a high-rank bituminous to anthracite coal with significant crystalline order, low aliphatic content, and well-developed aromatic structures. These characteristics make it suitable for applications where high thermal efficiency is required, such as in the production of hydrogen fuel using advanced technologies like Integrated Gasification Combined Cycle (IGCC) and Integrated Gasification Fuel Cell (IGFC).

Reference

Ajieh, M. U., Owamah, H. I., Edomwonyi-Otu, L. C., Ajieh, G. I., Aduba, P., Owebor, K., & Ikpeseni, S. C. (2023). Characteristics of fuelwood perturbation and effects on carbon monoxide and particulate pollutants emission from cookstoves in Nigeria. *Energy for Sustainable Development*, *72*, 151–161. https://doi.org/10.1016/j.esd. 2022.12.008

Banerjee, C., Chandaliya, V. K., Dash, P. S., & Meikap, B. C. (2019). Effect of different parameters on porosity and compressive strength of coal tar pitch derived carbon foam. *Diamond and Related Materials*, *95*, 83–90. https://doi.org/10.1016/j.diamond.2019.04.009

Chang, S., Zhuo, J., Meng, S., Qin, S., & Yao, Q. (2016). Clean Coal Technologies in China: Current Status and Future Perspectives. *Engineering*, *2*(4), 447–459. https://doi.org/10.1016/J.ENG.2016.04.015

Chen, W., & Xu, R. (2010). Clean coal technology development in China. *Energy Policy*, *38*(5), 2123–2130. https://doi.org/10.1016/j.enpol.2009.06.003

Clark, R., Zucker, N., & Urpelainen, J. (2020). The future of coal-fired power generation in Southeast Asia. *Renewable and Sustainable Energy Reviews*, *121*. https://doi.org/10.1016/j.rser.2019.109650

Costa, J. A. S., & Paranhos, C. M. (2020). Mitigation of silica-rich wastes: An alternative to the synthesis eco-friendly silica-based mesoporous materials. In *Microporous and Mesoporous Materials* (Vol. 309). Elsevier B.V. https://doi.org/10.1016/j.micromeso.2020.110570

Ezemonye, L. I. N., Ogbomida, E. T., & Ajieh, M. U. (n.d.). *Chapter Eight The Problem Of Energy Security In Africa: Prospects And Challenges*.

Franco, A., & Diaz, A. R. (2009). The future challenges for "clean coal technologies": Joining efficiency increase and pollutant emission control. *Energy*, *34*(3), 348–354. https://doi.org/10.1016/j.energy.2008.09.012

Gao, M., Yang, Z., Wang, Y., Bai, Y., Li, F., & Xie, K. (2017a). Impact of calcium on the synergistic effect for the reactivity of coal char gasification in H2O/CO2 mixtures. *Fuel*, *189*, 312–321. https://doi.org/10.1016/j.fuel.2016.10.100

Gao, M., Yang, Z., Wang, Y., Bai, Y., Li, F., & Xie, K. (2017b). Impact of calcium on the synergistic effect for the reactivity of coal char gasification in H2O/CO2 mixtures. *Fuel*, *189*, 312–321. https://doi.org/10.1016/j.fuel.2016.10.100

Ghose, M. K. (2009). Technological challenges for boosting coal production with environmental sustainability. *Environmental Monitoring and Assessment*, *154*(1–4), 373–381. https://doi.org/10.1007/s10661-008-0404-5

Hazra, B., Wood, D. A., Panda, M., Sethi, C., Vishal, V., Chandra, D., & Ostadhassan, M. (2025). Pore Structural Complexities and Gas Storage Capacity of Indian Coals with Various Thermal Maturities. *Energy and Fuels*. https://doi.org/10.1021/acs.energyfuels.5c00021

He, X., Liu, X., Nie, B., & Song, D. (2017). FTIR and Raman spectroscopy characterization of functional groups in various rank coals. *Fuel*, *206*, 555–563. https://doi.org/10.1016/j.fuel.2017.05.101

Hou, S., Wang, X., Wang, X., Yuan, Y., Pan, S., & Wang, X. (2017). Pore structure characterization of low volatile bituminous coals with different particle size and tectonic deformation using low pressure gas adsorption. *International Journal of Coal Geology*, *183*, 1–13. https://doi.org/10.1016/j.coal.2017.09.013

Jiang, J., Yang, W., Cheng, Y., Liu, Z., Zhang, Q., & Zhao, K. (2019a). Molecular structure characterization of middle-high rank coal via XRD, Raman and FTIR spectroscopy: Implications for coalification. *Fuel*, *239*, 559–572. https://doi.org/10.1016/j.fuel.2018.11.057

Jiang, J., Yang, W., Cheng, Y., Liu, Z., Zhang, Q., & Zhao, K. (2019b). Molecular structure characterization of middle-high rank coal via XRD, Raman and FTIR spectroscopy: Implications for coalification. *Fuel*, *239*, 559–572. https://doi.org/10.1016/j.fuel.2018.11.057

Jie, D., Xu, X., & Guo, F. (2021). The future of coal supply in China based on non-fossil energy development and carbon price strategies. *Energy*, *220*. https://doi.org/10.1016/j.energy.2020.119644

Kavouridis, K., & Koukouzas, N. (2008). Coal and sustainable energy supply challenges and barriers. *Energy Policy*, *36*(2), 693–703. https://doi.org/10.1016/j.enpol.2007.10.013

Li, K., Khanna, R., Zhang, J., Barati, M., Liu, Z., Xu, T., Yang, T., & Sahajwalla, V. (2015). Comprehensive Investigation of Various Structural Features of Bituminous Coals Using Advanced Analytical Techniques. *Energy and Fuels*, *29*(11), 7178–7189. https://doi.org/10.1021/acs.energyfuels.5b02064

Li, R., Tang, Y., Che, Q., Ma, P., Luo, P., Lu, X., & Dong, M. (2022). Effects of Coal Rank and Macerals on the Structure Characteristics of Coal-Based Graphene Materials from Anthracite in Qinshui Coalfield. *Minerals*, *12*(5). https://doi.org/10.3390/min12050588

Melikoglu, M. (2018). Clean coal technologies: A global to local review for Turkey. In *Energy Strategy Reviews*, 22,313–319).

Norouzi, N., Talebi, S., & Shahbazi, A. (2020). Chemical Review and Letters An overview on the carbon capture technologies with an approach of green coal production study. *Chem Rev Lett*, *3*, 65–78.

Oboirien, B. O., North, B. C., Obayopo, S. O., Odusote, J. K., & Sadiku, E. R. (2018). Analysis of clean coal technology in Nigeria for energy generation. *Energy Strategy Reviews*, *20*, 64–70. https://doi.org/10.1016/j.esr.2018.01.002

Okolo, G. N., Neomagus, H. W. J. P., Everson, R. C., Roberts, M. J., Bunt, J. R., Sakurovs, R., & Mathews, J. P. (2015a). Chemical-structural properties of South African bituminous coals: Insights from wide angle XRD-carbon fraction analysis, ATR-FTIR, solid state 13C NMR, and HRTEM techniques. *Fuel*, *158*, 779–792. https://doi.org/10.1016/j.fuel.2015.06.027

Okolo, G. N., Neomagus, H. W. J. P., Everson, R. C., Roberts, M. J., Bunt, J. R., Sakurovs, R., & Mathews, J. P. (2015b). Chemical-structural properties of South African bituminous coals: Insights from wide angle XRD-carbon fraction analysis, ATR-FTIR, solid state 13C NMR, and HRTEM techniques. *Fuel*, *158*, 779–792. https://doi.org/10.1016/j.fuel.2015.06.027

Oseni, M. O. (2011). An analysis of the power sector performance in Nigeria. In *Renewable and Sustainable Energy Reviews* (Vol. 15, Issue 9, pp. 4765–4774). Elsevier Ltd. https://doi.org/10.1016/j.rser.2011.07.075

Peteves, S. D., Kavalov, Boyan., & Institute for Energy (European Commission). (2007). *The future of coal*. Publications Office.

Pudasainee, D., Kurian, V., & Gupta, R. (2020a). Coal: Past, present, and future sustainable use. In *Future Energy: Improved, Sustainable and Clean Options for Our Planet* (pp. 21–48). Elsevier. https://doi.org/10.1016/B978-0-08-102886-5.00002-5

Pudasainee, D., Kurian, V., & Gupta, R. (2020b). Coal: Past, present, and future sustainable use. In *Future Energy: Improved, Sustainable and Clean Options for Our Planet* (pp. 21–48). Elsevier. https://doi.org/10.1016/B978-0-08-102886-5.00002-5

Qiao, L., Deng, C., Lu, B., Wang, Y., Wang, X., Deng, H., & Zhang, X. (2022). Study on calcium catalyzes coal spontaneous combustion. *Fuel*, *307*. https://doi.org/10.1016/j.fuel.2021.121884

Rawat, K., & Yadav, A. K. (2019). Characterization of coal and fly ash (generated) at coal based thermal power plant. *Materials Today: Proceedings*, *26*, 1406–1411. https://doi.org/10.1016/j.matpr.2020.02.292

Reddy, B. R., & Vinu, R. (2016). Microwave assisted pyrolysis of Indian and Indonesian coals and product characterization. *Fuel Processing Technology*, *154*, 96–103. https://doi.org/10.1016/j.fuproc.2016.08.016

Shoko, E., McLellan, B., Dicks, A. L., & da Costa, J. C. D. (2006). Hydrogen from coal: Production and utilisation technologies. *International Journal of Coal Geology*, *65*(3–4), 213–222. https://doi.org/10.1016/j.coal.2005.05.004

Stiegel, G. J., & Ramezan, M. (2006). Hydrogen from coal gasification: An economical pathway to a sustainable energy future. *International Journal of Coal Geology*, *65*(3–4), 173–190. https://doi.org/10.1016/j.coal.2005.05.002

Takeshita, T., & Yamaji, K. (n.d.). *Environmental Economics and Policy Studies Potential contribution of coal to the future global energy system*.

van der Zwaan, B. (2005). Will coal depart or will it continue to dominate global power production during the 21st century? In *Climate Policy*, 5(4), 445–453). https://doi.org/10.1080/14693062.2005.9685569

Yan, J., Lei, Z., Li, Z., Wang, Z., Ren, S., Kang, S., Wang, X., & Shui, H. (2020). Molecular structure characterization of low-medium rank coals via XRD, solid state 13C NMR and FTIR spectroscopy. *Fuel*, *268*. https://doi.org/10.1016/j.fuel.2020.117038

Yan, J., Yang, Q., Zhang, L., Lei, Z., Li, Z., Wang, Z., Ren, S., Kang, S., & Shui, H. (2020). Investigation of kinetic and thermodynamic parameters of coal pyrolysis with model-free fitting methods. *Carbon Resources Conversion*, *3*, 173–181. https://doi.org/10.1016/j.crcon.2020.11.002

Yan, Y. G., Mao, Z. J., Luo, J. J., Du, R. P., & Lin, J. X. (2020). Simultaneous removal of SO2, NOx and Hg0 by O3 oxidation integrated with bio-charcoal adsorption. *Ranliao Huaxue Xuebao/Journal of Fuel Chemistry and Technology*, *48*(12), 1452–1460. https://doi.org/10.1016/s1872-5813(20)30092-x

Yang, F., & Qiu, D. (2019). Exploring coal spontaneous combustion by bibliometric analysis. *Process Safety and Environmental Protection*, *132*, 1–10. https://doi.org/10.1016/j.psep.2019.09.017

Yegulalp, T. M., Lackner, K. S., & Ziock, H. J. (2001). A review of emerging technologies for sustainable use of coal for power generation. *International Journal of Surface Mining, Reclamation and Environment*, *15*(1), 52–68. https://doi.org/10.1076/ijsm.15.1.52.3423

Zhang, X., Winchester, N., & Zhang, X. (2017). The future of coal in China. *Energy Policy*, *110*, 644–652.